

Self-Supervised Representation Learning from Flow Equivariance

Yuwen Xiong Mengye Ren Wenyuan Zeng Raquel Urtasun
 Uber ATG University of Toronto
 {yuwen, mren, wenyuan, urtasun}@cs.toronto.edu

Abstract

Self-supervised representation learning is able to learn semantically meaningful features; however, much of its recent success relies on multiple crops of an image with very few objects. Instead of learning view-invariant representation from simple images, humans learn representations in a complex world with changing scenes by observing object movement, deformation, pose variation, and ego motion. Motivated by this ability, we present a new self-supervised learning representation framework that can be directly deployed on a video stream of complex scenes with many moving objects. Our framework features a simple flow equivariance objective that encourages the network to predict the features of another frame by applying a flow transformation to the features of the current frame. Our representations, learned from high-resolution raw video, can be readily used for downstream tasks on static images. Readout experiments on challenging semantic segmentation, instance segmentation, and object detection benchmarks show that we are able to outperform representations obtained from previous state-of-the-art methods including SimCLR [5] and BYOL [18].

1. Introduction

Rich and informative visual representations epitomize the revolution of deep learning in computer vision in the past decade. Deep neural nets deliver surprisingly competitive performance on tasks such as object detection [15, 36, 8] and semantic segmentation [4, 53]. Until very recently, visual representations have been learned by large scale supervised learning. Compared to object classification however, it is much more expensive to obtain labels for semantic or instance segmentation tasks. On the other hand, the human brain learns generic visual representations from raw videos of the complex world without much explicit supervision. This is the direction that we would like to get one step closer towards in this paper.

Recent advances in self-supervised or unsupervised representation learning, such as SimCLR [5] and BYOL [18],

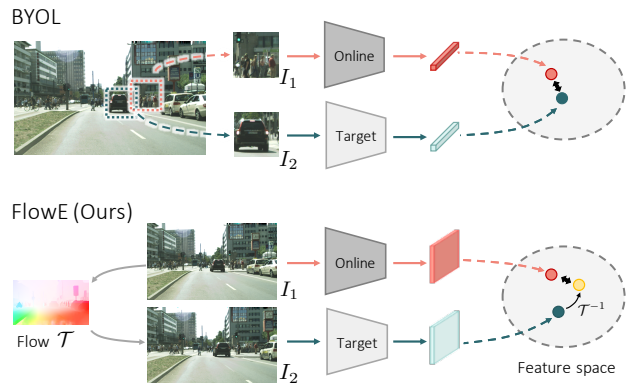


Figure 1: Our proposed self-supervised representation learning from Flow Equivariance (FlowE). Our method is based on BYOL [18], a state of the art method for static image representation learning. We encourage the features to obey the same flow transformation as the input image pairs.

seem to point us to a bright path forward: by simply minimizing the feature distance between two different views of a single image, and performing linear readout at test time on top, state-of-the-art approaches are now able to match the classification performance of networks trained with full supervision end-to-end [25, 38, 22]. While not using any class labels, these methods still rely on the dataset curation process of carefully selecting clean and object-centered images with a balanced class distribution. In contrast, videos in the wild feature crowded scenes and severe data imbalance. As a result, different crops of the same frame can often lead to either uninteresting regions or erroneous alignment of different instances in crowded areas. Moreover, none of these methods leverage temporal information, which contains a rich set of object movement, deformation, and pose variations. While there has been a large body of literature on learning representation from video [46, 26, 47, 37, 12, 13, 44, 45], they typically focus on predicting correspondence across frames and have not shown better performance on generic downstream tasks such as semantic and instance segmentation than pretrained supervised representations from ImageNet [21].

In this paper, we are interested in learning generic representations from raw high-resolution videos that are directly useful for object detection as well as semantic and instance segmentation. Whereas prior invariance-based learning algorithms completely disregard ego-motion and flow transformations across frames, we argue these are essential elements responsible for the learning of visual representations in complex scenes [1]. Instead of enforcing multiple crops of the same image (or adjacent frames) to be close in the feature space, as advocated in prior literature [19, 5, 18, 16], we propose a simple flow equivariance objective that can be applied densely at every pixel on the feature map, summarized in Figure 1. In particular, given two consecutive video frames, we estimate an optical flow map that denotes a pixel-wise transformation \mathcal{T} between the two frames. We then train the network to minimize the distance between the first frame \mathbf{h}_1 and the warped features of the second frame $\mathcal{T}^{-1}(\mathbf{h}_2)$. Using optical flow ensures that crowded regions are handled with precise instance alignment. It is also worth noting that off-the-shelf flow estimators can be trained from either graphics simulation [2, 11, 28] or ego-motion and depth estimation [35], without any human labeling effort.

Experiments are carried out on two complex driving video datasets, BDD100K [51] and our in-house dataset UrbanCity, which are collected from a front camera on a moving car, just like seeing from a mobile agent in the wild. Our approach, learning from raw videos, can achieve competitive readout performance on semantic and instance segmentation tasks, while invariance-based methods such as BYOL fail. Surprisingly, we are also able to outperform pre-trained representations from ImageNet [22], likely because of the large domain gap between ImageNet and driving videos.

2. Related Work

In the past few years, there has been tremendous progress in learning visual representations without class label supervision [17]. Typically, networks are trained to predict certain held-out information about the inputs, such as context [9, 30], rotation [14], colorization [52] and counting [31]. Although they have shown to learn interesting representations, they are still significantly behind supervised representations on classification tasks.

More recently, contrastive learning [32, 43] has emerged as a promising direction for representation learning, closing the gap with supervised representation on ImageNet. The high-level idea is to obtain different views of the same image using random cropping and other data augmentations to serve as positive labels, contrasting with other images that serve as negative labels. MoCo [19] proposed to perform momentum averaging on the network that encodes negative samples, and SimCLR [5] proposed to add a decoder to make the core representation more general.

Building along this line of work, BYOL [18] removed

the need for negative samples by simply minimizing the feature distance between a pair of views of the same image, which significantly reduced the batch size needed for contrastive learning. To make feature augmentation more diverse, it also encodes the second view with a slow network whose weights are getting slowly updated from the fast network. It is currently the state-of-the-art method for representation learning on ImageNet. However, all of the above methods rely on clean static images, which cannot be easily obtained through raw videos.

Applying contrastive learning on videos seems like a direct extension. [46] proposed to perform unsupervised tracking first to obtain positive and negative crops of images from different frames in a video sequence. [37] proposed a multi-view approach that tries to learn by matching different views from multiple cameras. More recently, [33] treated adjacent frames as positive pairs, whereas [34] pre-processed videos by a class agnostic object detector. [16] proposed multi-label video contrastive learning. While using video as input, these methods only consider the invariance relation between frames and throw away transformations across frames.

This drawback could potentially be complemented by another class of self-supervised learning algorithms that aim to predict some level of correspondence or transformation across frames [1, 26]. Cycle consistency is a popular form of self-supervision that encourages both forward and backward flow on a sequence of frames to be consistent [47, 24]. [12] looked at frame-wise correspondence across different videos. Typically these approaches show competitive performance in terms of video correspondence and label propagation [47, 24], demonstrating a rough understanding of optical flow. In fact, flow correspondence itself could also be used as feature representations for action recognition in the early literature [44, 45]. Distinctive to all the approaches above, in our work, we would like to decouple the two tasks of 1) predicting flow correspondence and 2) learning generic visual representation, by providing the network with off-the-shelf flow estimation.

There has also been a large body of literature on equivariance learning. Just like how the convolution operator is translational equivariant, [29, 6, 48] enforce strict equivariance over transformation groups. In comparison, we do not enforce strict equivariance but instead embed equivariance in our training objective to achieve self-supervision. Our work is most similar to [42] which also warps feature maps using optical flow [55, 54]. Whereas [42] tried to directly regress the relative coordinates, we make use of a simpler distance loss in the feature space. In the end, [42] produced a 3-dimensional image encoding and by contrast we produce generic high dimensional visual representations, readily usable for challenging downstream tasks.

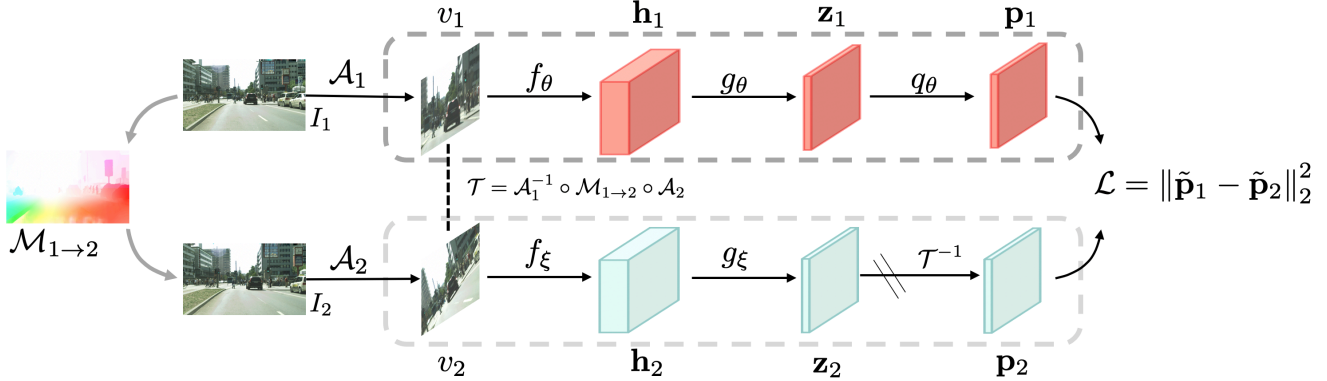


Figure 2: The overall learning procedure of FlowE. Given two adjacent video frames I_1 and I_2 , and two independent data augmentations \mathcal{A}_1 and \mathcal{A}_2 , a standalone flow network predicts a dense optical flow field $\mathcal{M}_{1 \rightarrow 2}$. The two augmented version of images are then fed into the online and target neural network respectively. Unlike BYOL, the intermediate features \mathbf{h} , \mathbf{z} and \mathbf{p} contain the spatial dimensions. The inverse transformation \mathcal{T}^{-1} is used to warp \mathbf{z}_2 to \mathbf{p}_2 to make it align with \mathbf{p}_1 . $\tilde{\cdot}$ denotes normalized activations.

3. Models

3.1. Background

In the background section, we first review BYOL, a state-of-the-art self-supervised representation learning algorithm. Our algorithm will build upon BYOL. Then we cover the basics of flow warping.

Bootstrap your own latent (BYOL): BYOL performs representation learning by matching two different views of the same image together. It consists of two neural networks: the online and target networks. The online network gets updated every iteration and the target network keeps a momentum averaged copy of the weights. During training, the online network is going to predict the features produced by the target network, and the motivation of having a separate target network is to avoid trivial solutions where all images collapse to the same representation.

More specifically, two augmented views v_1 and v_2 of the same sample are fed into the encoder f of the online and target network, to get representation $\mathbf{h}_1, \mathbf{h}_2$. In order to keep the representations general for other readout tasks, BYOL adds a projector g just like the decoder in SimCLR [5] and obtain corresponding projection \mathbf{z}_1 and \mathbf{z}_2 . Finally, the predictor q takes \mathbf{z}_1 and try to produce \mathbf{p}_1 that matches with \mathbf{z}_2 . Concretely, BYOL maximizes the cosine similarity between \mathbf{p}_1 and \mathbf{z}_2 , and the loss function defined as:

$$\mathcal{L} = \|\tilde{\mathbf{p}}_1 - \tilde{\mathbf{z}}_2\|_2^2, \quad (1)$$

where $\tilde{\cdot}$ denotes unit-normalization. Note that the target network is only updated through moving average to avoid trivial solutions of collapsed representation. After the self-supervised training is finished, the projector and predictor of the online network as well as the target network are dis-

carded and the encoder of the online network will be preserved for further readout of downstream tasks such as object classification.

Warping via optical flow: Optical flow is widely used in many video analysis and processing applications. A flow field is a two-dimensional vector field which defines dense pixel correspondences between two different video frames. Given a flow field $\mathcal{M}_{1 \rightarrow 2}$, for each pixel on I_1 we can find the corresponding location on I_2 and obtain the pixel value via bilinear interpolation. The warping operation can also be applied to convolutional feature maps [55, 54]. In our work, we use an off-the-shelf optical flow predictor RAFT [41] because of its empirical success.

3.2. Learning from Flow Equivariance

Our method learns dense pixel-level representation based on a flow equivariance objective, which encourages the features to obey the same flow transformation as the input image pairs. Our equivariance objective ensures that the positive pair of examples are sampled from the same object across two different video frames.

Fig. 2 shows the overview of our framework. Next, we will explain how it works in detail.

Optical flow & random affine transformation: Given two images I_1 and I_2 from a video, We use a frozen flow network \mathcal{F} to predict a dense optical flow field $\mathcal{M}_{1 \rightarrow 2}$ from the two images. We then obtain augmented versions of the two images by performing random affine transformations \mathcal{A}_1 and \mathcal{A}_2 :

$$v_1 = \mathcal{A}_1(I_1) \quad (2)$$

$$v_2 = \mathcal{A}_2(I_2). \quad (3)$$

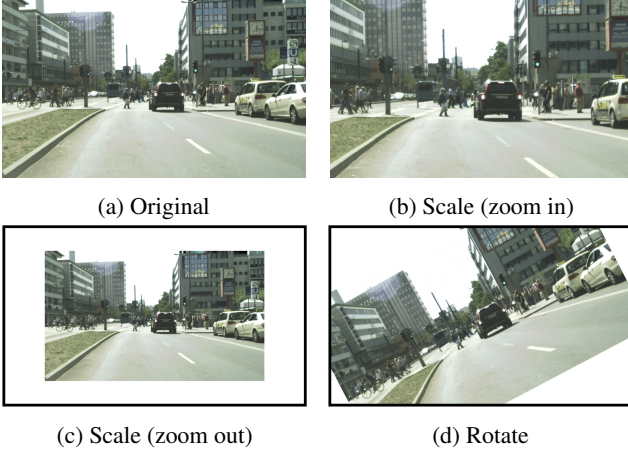


Figure 3: Random affine transformations. We consider adding random scaling and rotation before sending the images to the network.

Following [5, 18], we further apply random color distortion and Gaussian blurring on each image. The flow transformation \mathcal{T} between v_1 and v_2 is thus defined as the following:

$$\mathcal{T} = \mathcal{A}_1^{-1} \circ \mathcal{M}_{1 \rightarrow 2} \circ \mathcal{A}_2. \quad (4)$$

We then feed the two views into an online network f_θ, g_θ and a momentum updated network f_ξ, g_ξ to obtain the representation $\mathbf{h}_1, \mathbf{h}_2$, projection $\mathbf{z}_1, \mathbf{z}_2$ and prediction \mathbf{p}_1 , as shown in Fig. 2.

Equivariance learning: Our network is fully convolutional and the spatial dimension of the feature maps are preserved to represent multiple objects for complex video scenes. We propose to use equivariance as our training objective. Concretely, we use the inverse flow \mathcal{T}^{-1} to warp back \mathbf{z}_2 to obtain $\tilde{\mathbf{p}}_2 = \mathcal{T}^{-1}(\mathbf{z}_2)$. We use the online network output \mathbf{p}_1 from the predictor to match with $\tilde{\mathbf{p}}_2$. The objective is simply a squared ℓ_2 loss averaged over all spatial locations.

$$\mathcal{L} = \frac{1}{HW} \|\tilde{\mathbf{p}}_1 - \tilde{\mathbf{p}}_2\|_2^2, \quad (5)$$

where $\tilde{\cdot}$ denotes the unit-normalization across the channel dimension, and H and W denote the spatial resolution of the convolutional feature map. Similar to the loss in Equation 1, we make sure that every pixel pair in p_1 and p_2 has high cosine similarity.

Full Algorithm: The full learning algorithm is summarized in Algorithm 1, in PyTorch style.

3.3. Implementation Details

Network architecture: We use ResNet-50 as our base encoder network with larger output resolution. Following

Algorithm 1 Pseudocode in a PyTorch-like style.

```

for I1, I2 in data_loader:
    with no_grad():
        flow = flownet(I1, I2) # [B, 2, H, W]

    v1, A1 = data_aug(I1)
    v2, A2 = data_aug(I2)

    h1 = encoder(v1) # f_theta
    z1 = projector(h1) # g_theta
    p1 = predictor(z1) # q_theta

    with no_grad():
        h2 = target_encoder(v2) # f_xi
        z2 = target_decoder(h2) # g_xi

    # upsample to match flow shape
    p1 = upsample(p1) # [B, C, H, W]
    z2 = upsample(z2) # [B, C, H, W]

    # warp the feature map with flow via bilinear interp
    inv_T = apply(apply(inv(A1), flow), A2)
    p2 = transform(z2, inv_T)

    l = loss(normalize(p1), normalize(p2)) # Eq. (5)
    l.backward()

    optimizer.update([encoder, projector, predictor])
    momentum_update([target_encoder, target_decoder])

```

[53], we use dilated convolution [3] and remove the down-sampling operation in the last two stages, resulting in an encoder with output stride 8. The number of channels in the projector and predictor are the same as BYOL [18]. To preserve the spatial dimensions of the output feature maps, we first remove the final global average pooling layer in the encoder f . The linear layers in the following projector g and predictor q are also replaced with 1×1 convolutional layers to handle the convolutional feature maps, which do not introduce any extra parameters comparing to the original BYOL.

Flow network: For optical flow prediction, we use RAFT [41] as an off-the-shelf solution. The model is trained on Flying Chair [11], Flying Things [28] and Sintel [2] datasets. All of these datasets contain only synthetic data with no human labeling. The network is kept frozen during our experiments.

Data augmentation: For color distortion and Gaussian blurring, we use the same parameters as the ones used in SimCLR [5]. For affine transformation, we perform random scaling between $0.5 \sim 2.0\times$ and rotation between $-30 \sim 30$ degrees.

Flow post-processing: Since the affine transformation and flow operation are not strictly bijective due to cropping and object occlusion, in the loss function we ignore any pixels that have no correspondence. Occluded pixels can be found by a forward-backward flow consistency check [40].

Method	UrbanCity				BDD100K			
	mIoU	mAP	mIoU [†]	mAP [†]	mIoU	mAP	mIoU [†]	mAP [†]
Rand Init	9.4	0.0	27.3	6.4	9.8	0.0	22.0	5.5
BYOL [18]	14.0	0.0	19.6	5.0	11.3	0.0	21.9	4.5
BYOL (crop)	13.5	0.0	26.6	5.1	9.5	0.0	18.2	4.2
BYOL (crop w/ video)	7.8	0.0	13.0	2.0	8.2	0.0	10.7	2.1
CRW [24]	19.0	0.0	31.6	15.2	19.4	1.7	34.7	22.9
VINCE [16]	30.6	0.9	47.4	17.8	23.2	0.1	39.5	23.8
FlowE (Ours)	49.6	5.8	61.7	19.0	37.6	5.8	49.8	24.9
End-to-end supervised	63.3	2.2	67.0	16.5	52.0	8.0	56.6	20.0

Table 1: Self-supervised learning results on UrbanCity and BDD100K. All readouts are done with a frozen backbone except for the “end-to-end supervised” entry.

Method	Train data	UrbanCity				BDD100K			
		mIoU	mAP	mIoU [†]	AP [†]	mIoU	mAP	mIoU [†]	mAP [†]
Supervised	ImageNet	39.6	3.3	57.7	18.8	34.0	3.6	52.4	24.9
SimCLR [5]	ImageNet	37.0	3.0	58.6	21.0	28.1	2.7	51.0	26.8
BYOL [18]	ImageNet	35.4	2.4	59.8	19.5	28.3	2.8	52.4	26.0
VINCE [16]	R2V2	23.6	1.2	57.4	18.1	19.4	1.4	47.0	24.2
FlowE (Ours)	-	49.6	5.8	61.7	19.0	37.6	5.8	49.8	24.9

Table 2: Readout comparisons to competitive representation learning methods trained on other data sources.

4. Experiments

We train our model on two self-driving datasets UrbanCity and BDD100K [51]. To evaluate the quality of the learned representation, we target object detection, instance segmentation, and semantic segmentation as readout tasks on the two datasets with labeled images. We further test the transferability of the learned feature by solely performing readout experiments on the Cityscapes dataset [7] with models trained on UrbanCity and BDD100K. Ablation experiments are conducted on UrbanCity to verify the effectiveness of each component of our model.

4.1. Datasets

UrbanCity dataset: UrbanCity is an in-house large-scale self-driving dataset collected by ourselves. It contains around 15,000 video snippets where each is about 25 seconds long at 1080p and 10 fps, with a total of 3.5 million frames. Within these, 11,580 and 1,643 images are densely labeled, for training and validation respectively. They contain 7 instance classes: bicycle, motorcycle, movable object, pedestrian, bus, car, construction vehicle, train, truck, and 13 semantic classes: building, cone, curb, pole, road, sidewalk, sky, traffic sign, traffic light (front), traffic light (not front), and vegetation. We uniformly sampled 256,000 frames with a 0.4 second time interval. In the readout setting, we use the annotated train and val split to perform semantic and instance segmentation tasks.

BDD100K dataset: BDD100K [51] is a large-scale self-driving dataset which contains 100,000 unlabeled raw video

snippets for street scene, where each is about 40 seconds long at 720p and 30 fps. It captures different weather conditions, including sunny, overcast, and rainy, as well as different times of day including nighttime. The class definition is the same as Cityscapes [7] which consists of 8 instance classes for object detection, and 19 classes in total for semantic segmentation. 7,000 train and 1,000 val images are densely labeled for semantic segmentation; 70,000 train, 10,000 val images are labeled for object detection. We use the 70,000 video snippets in the official training split to perform self-supervised learning. At each iteration, we randomly sample a pair of frames with a 0.5 second time interval. For evaluation, we use the annotated images to perform readout experiments on semantic segmentation and object detection.

4.2. Experimental Setup

FlowE: We use 64 GPUs with 2 pairs of frames per GPU, leading to a total mini-batch size 128. LARS [50] optimizer is used with a cosine decay learning rate schedule [27] without restarts and an initial learning rate 0.1 with weight decay $1e-6$. The setting of the exponential moving average parameter of the target network is kept the same as the original BYOL paper. For UrbanCity, we will randomly scale the image pairs from $0.75 \sim 1.25\times$, and randomly crop a 512×1024 patch pair at the same location of the two images; models are run for 160,000 iterations (80 epochs). For BDD100K, we first upsample the images to be 1080×1920 , and follow the same setting for UrbanCity; model is run for

60,000 iterations (110 epochs), and it is worth noting that the performance has not saturated and longer iteration may yield better performance.

Readout setup: For semantic segmentation task, we train models for 60,000 iterations by SGD with mini-batch size 16, an initial learning rate 0.02 and the “poly” learning rate decay schedule [4] on both datasets, patches with 512×1024 are randomly cropped from images that are randomly resized with shorter side from 512 to 2048.

For instance segmentation task on UrbanCity, we train models for 32 epochs by SGD with mini-batch size 8 and an initial learning rate 0.01 with a decay factor 0.1 at epoch 28, multi-scale training is used with shorter side from 800 to 1024.

For object detection task on BDD100K we train models for 12 epochs by SGD with mini-batch size 16 and an initial learning rate 0.02 with a decay factor 0.1 at epoch 8 and 11, respectively, we keep the image resolution as it is and do not apply multi-scale training.

Standard readout header: In our readout setting, the encoder is frozen and only the newly added layer is trained. To better reflect the ability of the learned representation itself, we would like to mimic the linear evaluation protocol on ImageNet [19, 23, 10, 43, 49, 5, 18] and add as few parameters as possible. So that we use DeepLab v1 [3] as our semantic segmentation model as it has no extra heavy header. Besides dilated convolutions are used in the encoder, only one convolutional layer is added on top of the encoder to output per-pixel classification logits.

Similarly, for object detection on BDD100K, we use Faster R-CNN with ResNet-C4 architecture which is proposed in [22]. Only a small number of parameters are introduced: a small convnet RPN [36] and two linear layers for bounding box classification and regression.

For instance segmentation on UrbanCity, the same ResNet-C4 architecture is used with two more convolutional layers added for instance mask prediction as was done in [21].

Heavier readout header: While we believe that standard readout headers should be treated as our main evaluation metric for the quality of representations since there are less number of extra parameters, they may not be capable enough to capture the complex output structure for semantic and instance segmentation. To provide stronger comparisons, following LoCo [49], we also perform readout with a *heavier header* such DeepLabV3 decoder and FPN-style Faster and Mask R-CNN, where results obtained with these models are denoted with $mIoU^\dagger$ and mAP^\dagger .

4.3. Main Results

Results trained on UrbanCity and BDD100K: The results on UrbanCity and BDD100K are shown in Table 1.

We compare FlowE with various baselines, including Random initialization (readout from a random projection), BYOL [18], VINCE [16] and CRW [24] and our method is able to surpass them by a large margin. We analyze the competitive methods below:

BYOL: We first try to directly adapt BYOL [18] on our video data. For the simplest variant, we treat video frames like ImageNet images. The random crop augmentation has no constraint thus two crops from the same image may cover different objects. We can see that the performance is as poor as a randomly initialized encoder, indicating that the model has learned no meaningful representations.

We then try to crop a smaller patch on the original image to limit the movement of the random crop, denoted as “BYOL (crop)”. However, the performance is not good either. Furthermore, we also try BYOL using two neighboring video frames, *i.e.* BYOL (crop w/ video), but it is even worse due to extra object movement across frames. These results suggest that invariance-based objectives in popular SimCLR/BYOL frameworks might not be ideal for raw driving videos.

CRW: We also compared with CRW [24], a self-supervised approach to learn representations for visual correspondence. We use 5 frames with a 0.1 second time interval as inputs and follow the hyperparameters described in their paper. CRW has poor performance on semantic segmentation since it focuses on video correspondence as its training objective, and different classes of static objects cannot not be easily differentiated.

VINCE: VINCE [16] is one of the latest video representation learning methods that leverages a multi-label contrastive objective. We use inputs of 4 frames with a 0.1 second time interval. We can see that VINCE can learn some useful features from video data. However, our method is still significantly better.

Results trained on other data: We also compare FlowE with methods trained on other datasets, including supervised learning, SimCLR [5] and BYOL [18] on ImageNet, and VINCE [16] on R2V2 [16]. We simply freeze the pre-trained model weights and perform readout experiments on UrbanCity and BDD100K. For the supervised learning baseline, we use the ResNet-50 checkpoint provided by torchvision¹. For SimCLR, we use our own implementation and train a model that can obtain 69.8% top-1 accuracy on ImageNet. For BYOL and VINCE, we use weights released online by the authors. Our method can outperform or stay on par with other strong baselines in most cases, especially when using a standard readout header.

¹<https://download.pytorch.org/models/resnet50-19c8e357.pth>

Method	Train data	mIoU	mAP	mIoU [†]	mAP [†]
Supervised	ImageNet	43.8	6.1	59.9	25.3
SimCLR	ImageNet	39.9	5.0	60.3	28.9
BYOL	ImageNet	38.2	4.1	59.8	27.4
VINCE	R2V2	26.7	1.1	57.5	25.6
FlowE (Ours)	BDD100K	45.6	5.7	56.6	26.8
FlowE (Ours)	UrbanCity	51.1	7.4	63.7	28.1

Table 3: Readout results on Cityscapes with models trained on other datasets.

Pixel based	Affine transform	Video	mIoU	mAP	mIoU [†]	mAP [†]
✓			21.3	0.7	40.1	12.3
✓	✓		28.7	2.7	45.9	15.1
✓		✓	37.3	3.3	51.9	16.2
	✓	✓	17.8	0.7	33.1	10.9
✓	✓	✓	37.9	3.8	53.2	16.5

Table 4: Semantic segmentation and instance segmentation readout results on UrbanCity, the left part indicates different design choices we use during training.

4.4. Representation Transferability

We further test the transferability of the learned representation of FlowE by performing semantic and instance segmentation readout experiments on the Cityscapes dataset [7]. Our models are pretrained on UrbanCity and BDD100K. Following the common practice, for instance segmentation we train 64 epochs with mini-batch size 8, an initial learning rate 0.01 decayed by a factor of 10 at 56 epoch; for semantic segmentation, we train 40,000 iterations with a mini-batch size 8, an initial learning rate 0.01 with the ‘‘poly’’ learning rate decay schedule. The results are shown in Table 3. Our pretrained representations can be easily transferred to other driving dataset, and in most cases they are better than ImageNet pretrained representations.

4.5. Ablation Studies

We perform ablation studies are shown in Table 4. All entries are trained with 16K iterations for faster experimentation. When bringing video data with flow matching, we can see a huge performance improvement, indicating the importance of the equivariance objective derived from videos. For non pixel-based variant, we use a global average pooling after the encoder and get vector representation. Its poor performance on the readout tasks suggests the necessity of keeping the spatial dimension of the representation. Random affine transformation can also bring some additional gains. Finally, our full model achieves the best performance.

To test the generalizability and robustness of our framework, here we also experiment with a weaker flow model which produces worse flow prediction. Specifically, we use PWC-Net [39] which is pretrained on the same datasets as RAFT, *i.e.* Flying-chair, Flying-things and Sintel. Following ablation experiments in the main paper, we train our model on UrbanCity for 16K iterations. Shown in Table 5,

Flow model	mIoU	mAP	mIoU [†]	mAP [†]
PWC-Net	37.2	3.9	52.4	16.4
RAFT (main paper)	37.9	3.8	53.2	16.5

Table 5: Semantic segmentation and instance segmentation readout results on UrbanCity with a weaker flow model PWC-Net [39]

% of labels	1%	10%	100%
End-to-end supervised	42.0	59.5	63.3
FlowE (Ours)	53.9	64.0	68.8

Table 6: Semantic segmentation results on UrbanCity with limited labeled data,

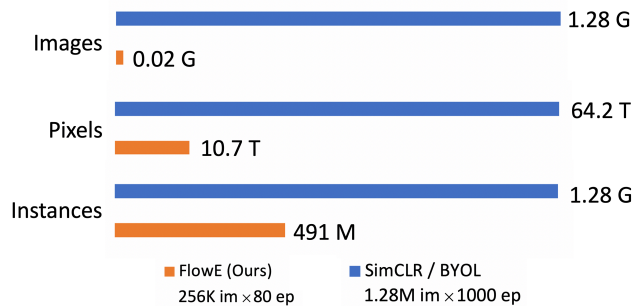


Figure 4: Total numbers of images, pixels, and instances seen during training. We count instances in ImageNet as 1 per image, while estimates instances in UrbanCity as 24 per image from the annotated images, and pixels in ImageNet as 224×224 and UrbanCity as 512×1024 . FlowE achieves better sample efficiency.

using a weaker flow model in our framework only has a minor impact on model performance.

We further conduct experiments on limited labeled data. We randomly subsample 1%, 10% on UrbanCity, fully finetune our model and compare it with the end-to-end supervised learning model on semantic segmentation with standard header (one 1×1 convolutional layer). The results are shown in Table 6. When finetuning is also enabled for our model, it can surpass the end-to-end supervised model, and the performance gap becomes larger when the number of samples decreases.

4.6. Sample Efficiency

We want to highlight that our method has a higher sample efficiency than other methods trained on ImageNet, possibly due to training on target domain datasets directly and training with pixel-level self-supervision which capture multiple objects at the same time. Following [20], we consider three definitions of ‘samples’ – the number of images, pixels and instances the network sees during training and count them for models trained on UrbanCity and ImageNet. From Fig. 4, our method can be on par or surpass baselines trained on ImageNet with less samples during training, which indicates a faster convergence speed of our model.

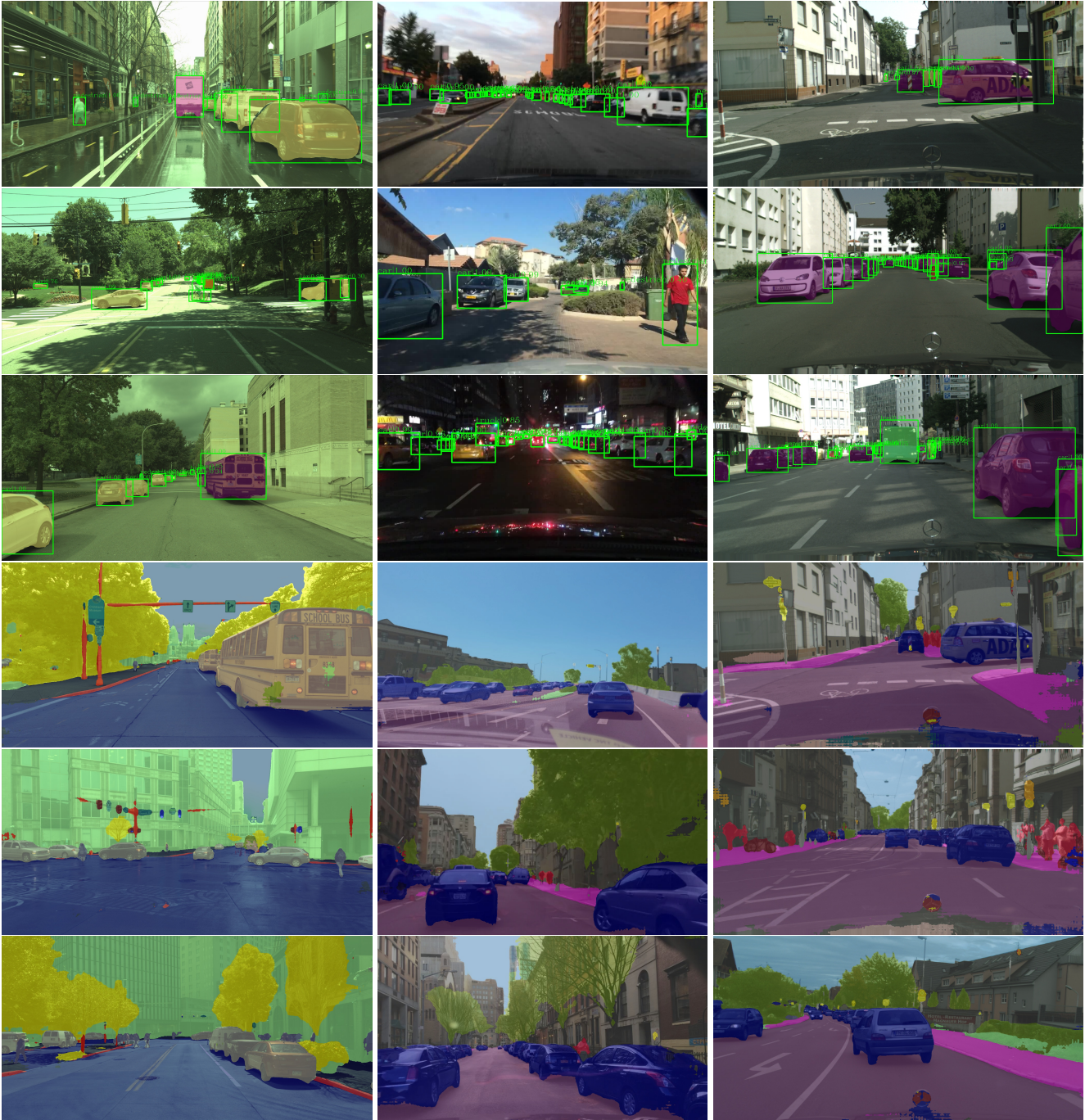


Figure 5: We show visualizations of instance segmentation / object detection (row 1-3) and semantic segmentation (row 4-6) readout results on UrbanCity (left), BDD100K [51] (middle), and Cityscapes [7] (right).

4.7. Visualization

We show the visualization results of UrbanCity, BDD100K [51] as well as Cityscapes [7] in Fig. 5. The first three rows show instance segmentation / object detection results and the last three rows show semantic segmentation results. For UrbanCity and BDD100K, models are trained

on the corresponding dataset. For Cityscapes, we use an UrbanCity pretrained model. We showcase results using the heavier header for instance segmentation and object detection, and the standard header for semantic segmentation.

4.8. Limitation

We observe that when using heavier readout headers instead of standard readout headers, the models trained on ImageNet are able to catch up with our model. We notice that in these cases our method performs much worse on instance classes like *rider* and *motorcycle*, which are usually rare in the datasets. This might be caused by the data imbalance when using our pixel-based objective, whereas ImageNet has a balanced distribution across semantic classes. Solely relying on equivariance objective and lack of invariance objectives may also sacrifice some higher-level representations.

5. Conclusion

We present a new self-supervised representation learning framework based on a flow equivariance objective. Our method is able to learn pixel-level representations from raw high-resolution videos with complex scenes. Large scale experiments on driving videos suggest that our unsupervised representations are useful for object detection, semantic and instance segmentation, and in many cases outperform state-of-the-art representations obtained from ImageNet.

References

- [1] Pulkit Agrawal, Joao Carreira, and Jitendra Malik. Learning to see by moving. In *Proceedings of the IEEE international conference on computer vision*, pages 37–45, 2015. 2
- [2] Daniel J Butler, Jonas Wulff, Garrett B Stanley, and Michael J Black. A naturalistic open source movie for optical flow evaluation. In *European conference on computer vision*, pages 611–625. Springer, 2012. 2, 4
- [3] Liang-Chieh Chen, George Papandreou, Iasonas Kokkinos, Kevin Murphy, and Alan L Yuille. Semantic image segmentation with deep convolutional nets and fully connected crfs. *arXiv preprint arXiv:1412.7062*, 2014. 4, 6
- [4] Liang-Chieh Chen, George Papandreou, Iasonas Kokkinos, Kevin Murphy, and Alan L Yuille. Deeplab: Semantic image segmentation with deep convolutional nets, atrous convolution, and fully connected crfs. *IEEE transactions on pattern analysis and machine intelligence*, 40(4):834–848, 2017. 1, 6
- [5] Ting Chen, Simon Kornblith, Mohammad Norouzi, and Geoffrey Hinton. A simple framework for contrastive learning of visual representations. *arXiv preprint arXiv:2002.05709*, 2020. 1, 2, 3, 4, 5, 6
- [6] Taco Cohen and Max Welling. Group equivariant convolutional networks. In *International conference on machine learning*, pages 2990–2999, 2016. 2
- [7] Marius Cordts, Mohamed Omran, Sebastian Ramos, Timo Rehfeld, Markus Enzweiler, Rodrigo Benenson, Uwe Franke, Stefan Roth, and Bernt Schiele. The cityscapes dataset for semantic urban scene understanding. In *Proceedings of the IEEE conference on computer vision and pattern recognition*, pages 3213–3223, 2016. 5, 7, 8
- [8] Jifeng Dai, Yi Li, Kaiming He, and Jian Sun. R-fcn: Object detection via region-based fully convolutional networks. In *Advances in neural information processing systems*, pages 379–387, 2016. 1
- [9] Carl Doersch, Abhinav Gupta, and Alexei A Efros. Unsupervised visual representation learning by context prediction. In *Proceedings of the IEEE international conference on computer vision*, pages 1422–1430, 2015. 2
- [10] Jeff Donahue and Karen Simonyan. Large scale adversarial representation learning. In *Advances in Neural Information Processing Systems*, pages 10542–10552, 2019. 6
- [11] Alexey Dosovitskiy, Philipp Fischer, Eddy Ilg, Philip Hausser, Caner Hazirbas, Vladimir Golkov, Patrick Van Der Smagt, Daniel Cremers, and Thomas Brox. FlowNet: Learning optical flow with convolutional networks. In *Proceedings of the IEEE international conference on computer vision*, pages 2758–2766, 2015. 2, 4
- [12] Debidatta Dwivedi, Yusuf Aytar, Jonathan Tompson, Pierre Sermanet, and Andrew Zisserman. Temporal cycle-consistency learning. In *Proceedings of the IEEE Conference on Computer Vision and Pattern Recognition*, pages 1801–1810, 2019. 1, 2
- [13] Debidatta Dwivedi, Yusuf Aytar, Jonathan Tompson, Pierre Sermanet, and Andrew Zisserman. Counting out time: Class agnostic video repetition counting in the wild. In *Proceedings of the IEEE/CVF Conference on Computer Vision and Pattern Recognition*, pages 10387–10396, 2020. 1
- [14] Spyros Gidaris, Praveer Singh, and Nikos Komodakis. Unsupervised representation learning by predicting image rotations. *arXiv preprint arXiv:1803.07728*, 2018. 2
- [15] Ross Girshick. Fast r-cnn. In *Proceedings of the IEEE international conference on computer vision*, pages 1440–1448, 2015. 1
- [16] Daniel Gordon, Kiana Ehsani, Dieter Fox, and Ali Farhadi. Watching the world go by: Representation learning from unlabeled videos, 2020. 2, 5, 6
- [17] Priya Goyal, Dhruv Mahajan, Abhinav Gupta, and Ishan Misra. Scaling and benchmarking self-supervised visual representation learning. In *Proceedings of the IEEE International Conference on Computer Vision*, pages 6391–6400, 2019. 2
- [18] Jean-Bastien Grill, Florian Strub, Florent Altché, Corentin Tallec, Pierre H Richemond, Elena Buchatskaya, Carl Doersch, Bernardo Avila Pires, Zhaohan Daniel Guo, Mohammad Gheshlaghi Azar, et al. Bootstrap your own latent: A new approach to self-supervised learning. *arXiv preprint arXiv:2006.07733*, 2020. 1, 2, 4, 5, 6
- [19] Kaiming He, Haoqi Fan, Yuxin Wu, Saining Xie, and Ross Girshick. Momentum contrast for unsupervised visual representation learning. In *Proceedings of the IEEE/CVF Conference on Computer Vision and Pattern Recognition*, pages 9729–9738, 2020. 2, 6
- [20] Kaiming He, Ross Girshick, and Piotr Dollár. Rethinking imagenet pre-training. In *Proceedings of the IEEE international conference on computer vision*, pages 4918–4927, 2019. 7

- [21] Kaiming He, Georgia Gkioxari, Piotr Dollár, and Ross Girshick. Mask r-cnn. In *Proceedings of the IEEE international conference on computer vision*, pages 2961–2969, 2017. 1, 6
- [22] Kaiming He, Xiangyu Zhang, Shaoqing Ren, and Jian Sun. Deep residual learning for image recognition. In *Proceedings of the IEEE conference on computer vision and pattern recognition*, pages 770–778, 2016. 1, 2, 6
- [23] Olivier J Hénaff, Aravind Srinivas, Jeffrey De Fauw, Ali Razavi, Carl Doersch, SM Eslami, and Aaron van den Oord. Data-efficient image recognition with contrastive predictive coding. *arXiv preprint arXiv:1905.09272*, 2019. 6
- [24] Allan Jabri, Andrew Owens, and Alexei A Efros. Space-time correspondence as a contrastive random walk. *arXiv preprint arXiv:2006.14613*, 2020. 2, 5, 6
- [25] Alex Krizhevsky, Ilya Sutskever, and Geoffrey E Hinton. Imagenet classification with deep convolutional neural networks. *Communications of the ACM*, 60(6):84–90, 2017. 1
- [26] Xueting Li, Sifei Liu, Shalini De Mello, Xiaolong Wang, Jan Kautz, and Ming-Hsuan Yang. Joint-task self-supervised learning for temporal correspondence. In *Advances in Neural Information Processing Systems*, pages 318–328, 2019. 1, 2
- [27] Ilya Loshchilov and Frank Hutter. Sgdr: Stochastic gradient descent with warm restarts. *arXiv preprint arXiv:1608.03983*, 2016. 5
- [28] Nikolaus Mayer, Eddy Ilg, Philip Hausser, Philipp Fischer, Daniel Cremers, Alexey Dosovitskiy, and Thomas Brox. A large dataset to train convolutional networks for disparity, optical flow, and scene flow estimation. In *Proceedings of the IEEE conference on computer vision and pattern recognition*, pages 4040–4048, 2016. 2, 4
- [29] Klas Nordberg and G. Granlund. Equivariance and invariance—an approach based on lie groups. *Proceedings of 3rd IEEE International Conference on Image Processing*, 3:181–184 vol.3, 1996. 2
- [30] Mehdi Noroozi and Paolo Favaro. Unsupervised learning of visual representations by solving jigsaw puzzles. In *European Conference on Computer Vision*, pages 69–84. Springer, 2016. 2
- [31] Mehdi Noroozi, Hamed Pirsiavash, and Paolo Favaro. Representation learning by learning to count. In *Proceedings of the IEEE International Conference on Computer Vision*, pages 5898–5906, 2017. 2
- [32] Aaron van den Oord, Yazhe Li, and Oriol Vinyals. Representation learning with contrastive predictive coding. *arXiv preprint arXiv:1807.03748*, 2018. 2
- [33] A Emin Orhan, Vaibhav V Gupta, and Brenden M Lake. Self-supervised learning through the eyes of a child. *arXiv preprint arXiv:2007.16189*, 2020. 2
- [34] Soeren Pirk, Mohi Khansari, Yunfei Bai, Corey Lynch, and Pierre Sermanet. Online learning of object representations by appearance space feature alignment. 2020. 2
- [35] Anurag Ranjan, Varun Jampani, Lukas Balles, Kihwan Kim, Deqing Sun, Jonas Wulff, and Michael J Black. Competitive collaboration: Joint unsupervised learning of depth, camera motion, optical flow and motion segmentation. In *Proceedings of the IEEE conference on computer vision and pattern recognition*, pages 12240–12249, 2019. 2
- [36] Shaoqing Ren, Kaiming He, Ross Girshick, and Jian Sun. Faster r-cnn: Towards real-time object detection with region proposal networks. In *Advances in neural information processing systems*, pages 91–99, 2015. 1, 6
- [37] Pierre Sermanet, Corey Lynch, Yevgen Chebotar, Jasmine Hsu, Eric Jang, Stefan Schaal, and Sergey Levine. Time-contrastive networks: Self-supervised learning from video. In *2018 IEEE International Conference on Robotics and Automation (ICRA)*, pages 1134–1141. IEEE, 2018. 1, 2
- [38] Karen Simonyan and Andrew Zisserman. Very deep convolutional networks for large-scale image recognition. *arXiv preprint arXiv:1409.1556*, 2014. 1
- [39] Deqing Sun, Xiaodong Yang, Ming-Yu Liu, and Jan Kautz. PWC-Net: CNNs for optical flow using pyramid, warping, and cost volume. In *IEEE Conf. Comput. Vis. Pattern Recog.*, 2018. 7
- [40] Narayanan Sundaram, Thomas Brox, and Kurt Keutzer. Dense point trajectories by gpu-accelerated large displacement optical flow. In *European conference on computer vision*, pages 438–451. Springer, 2010. 4
- [41] Zachary Teed and Jia Deng. Raft: Recurrent all-pairs field transforms for optical flow. *arXiv preprint arXiv:2003.12039*, 2020. 3, 4
- [42] James Thewlis, Hakan Bilen, and Andrea Vedaldi. Unsupervised learning of object frames by dense equivariant image labelling. In I. Guyon, U. V. Luxburg, S. Bengio, H. Wallach, R. Fergus, S. Vishwanathan, and R. Garnett, editors, *Advances in Neural Information Processing Systems 30*, pages 844–855. Curran Associates, Inc., 2017. 2
- [43] Yonglong Tian, Dilip Krishnan, and Phillip Isola. Contrastive multiview coding. *arXiv preprint arXiv:1906.05849*, 2019. 2, 6
- [44] Heng Wang, Alexander Kläser, Cordelia Schmid, and Cheng-Lin Liu. Action recognition by dense trajectories. In *CVPR 2011*, pages 3169–3176. IEEE, 2011. 1, 2
- [45] Heng Wang and Cordelia Schmid. Action recognition with improved trajectories. In *Proceedings of the IEEE international conference on computer vision*, pages 3551–3558, 2013. 1, 2
- [46] Xiaolong Wang and Abhinav Gupta. Unsupervised learning of visual representations using videos. In *Proceedings of the IEEE international conference on computer vision*, pages 2794–2802, 2015. 1, 2
- [47] Xiaolong Wang, Allan Jabri, and Alexei A Efros. Learning correspondence from the cycle-consistency of time. In *Proceedings of the IEEE Conference on Computer Vision and Pattern Recognition*, pages 2566–2576, 2019. 1, 2
- [48] Daniel Worrall and Gabriel Brostow. Cubenet: Equivariance to 3d rotation and translation. In *Proceedings of the European Conference on Computer Vision (ECCV)*, pages 567–584, 2018. 2
- [49] Yuwen Xiong, Mengye Ren, and Raquel Urtasun. Loco: Local contrastive representation learning. *arXiv preprint arXiv:2008.01342*, 2020. 6

- [50] Yang You, Igor Gitman, and Boris Ginsburg. Large batch training of convolutional networks. *arXiv preprint arXiv:1708.03888*, 2017. 5
- [51] Fisher Yu, Haofeng Chen, Xin Wang, Wenqi Xian, Yingying Chen, Fangchen Liu, Vashisht Madhavan, and Trevor Darrell. Bdd100k: A diverse driving dataset for heterogeneous multitask learning. In *Proceedings of the IEEE/CVF Conference on Computer Vision and Pattern Recognition (CVPR)*, June 2020. 2, 5, 8
- [52] Richard Zhang, Phillip Isola, and Alexei A Efros. Colorful image colorization. In *European conference on computer vision*, pages 649–666. Springer, 2016. 2
- [53] Hengshuang Zhao, Jianping Shi, Xiaojuan Qi, Xiaogang Wang, and Jiaya Jia. Pyramid scene parsing network. In *Proceedings of the IEEE conference on computer vision and pattern recognition*, pages 2881–2890, 2017. 1, 4
- [54] Xizhou Zhu, Yujie Wang, Jifeng Dai, Lu Yuan, and Yichen Wei. Flow-guided feature aggregation for video object detection. In *Proceedings of the IEEE International Conference on Computer Vision*, pages 408–417, 2017. 2, 3
- [55] Xizhou Zhu, Yuwen Xiong, Jifeng Dai, Lu Yuan, and Yichen Wei. Deep feature flow for video recognition. In *Proceedings of the IEEE conference on computer vision and pattern recognition*, pages 2349–2358, 2017. 2, 3